Journal of Nuclear Medicine, published on December 11, 2014 as doi:10.2967/jnumed.114.145995

# Toward Radioguided Surgery with $\beta^-$ Decays: Uptake of a Somatostatin Analogue, DOTATOC, in Meningioma and High-Grade Glioma

Francesco Collamati[1,2], Alessandra Pepe[3], Fabio Bellini[1,2], Valerio Bocci[2], Giacomo Chiodi[2], Marta Cremonesi[4], Erika De Lucia[5], Mahila E. Ferrari[4], Paola M. Frallicciardi[2,6], Chiara M. Grana[4], Michela Marafini[2,6], Ilaria Mattei[5,7], Silvio Morganti[2], Vincenzo Patera[2,3], Luca Piersanti[2,3], Luigi Recchia[2], Andrea Russomando[1,2,8], Alessio Sarti[5,3], Adalberto Sciubba[2,3], Martina Senzacqua[1,2], Elena Solfaroli Camillocci[8], Cecilia Voena[2], Davide Pinci[2], and Riccardo Faccini[1,2]

*[1]Dipartimento di Fisica, Sapienza Università di Roma, Roma, Italy; [2]INFN Sezione di Roma, Roma, Italy; [3]Dipartimento di Scienze di Base e Applicate per l'Ingegneria, Sapienza Università di Roma, Roma, Italy; [4]Istituto Europeo di Oncologia, Milano, Italy; [5]Laboratori Nazionali di Frascati dell'INFN, Frascati, Italy; [6]Museo Storico della Fisica e Centro Studi e Ricerche "E. Fermi," Roma, Italy; [7]Dipartimento di Fisica, Università RomaTre, Roma, Italy; and [8]Center for Life Nano Science@Sapienza, Istituto Italiano di Tecnologia, Roma, Italy*

A novel radioguided surgery (RGS) technique for cerebral tumors using $\beta^-$ radiation is being developed. Checking for a radiotracer that can deliver a $\beta^-$ emitter to the tumor is a fundamental step in the deployment of such a technique. This paper reports a study of the uptake of $^{90}$Y-DOTATOC in meningiomas and high-grade gliomas (HGGs) and a feasibility study of the RGS technique in these types of tumor. Estimates were performed assuming the use of a $\beta^-$ probe under development with a sensitive area 2.55 mm in radius to detect 0.1-mL residuals. **Methods:** Uptake and background from healthy tissues were estimated on $^{68}$Ga-DOTATOC PET scans of 11 meningioma patients and 12 HGG patients. A dedicated statistical analysis of the DICOM images was developed and validated. The feasibility study was performed using full simulation of emission and detection of the radiation, accounting for the measured uptake and background rate. **Results:** All meningioma patients but one with an atypical extracranial tumor showed high uptake of DOTATOC. In terms of feasibility of the RGS technique, we estimated that by administering a 3 MBq/kg activity of radiotracer, the time needed to detect a 0.1-mL remnant with 5% false-negative and 1% false-positive rates is less than 1 s. Actually, to achieve a detection time of 1 s the required activities to administer were as low as 0.2–0.5 MBq/kg in many patients. In HGGs, the uptake was lower than in meningiomas, but the tumor-to-nontumor ratio was higher than 4, which implies that the tracer can still be effective for RGS. It was estimated that by administering 3 mBq/kg of radiotracer, the time needed to detect a 0.1-mL remnant is less than 6 s, with the exception of the only oligodendroma in the sample. **Conclusion:** Uptake of $^{90}$Y-DOTATOC in meningiomas was high in all studied patients. Uptake in HGGs was significantly worse than in meningiomas but was still acceptable for RGS, particularly if further research and development are done to improve the performance of the $\beta^-$ probe.

**Key Words:** radioguided surgery; somatostatin analogue; meningioma; high-grade glioma

**J Nucl Med 2015; 56:1–6**
DOI: 10.2967/jnumed.114.145995

Radioguided surgery (RGS) helps the surgeon evaluate the completeness of a tumor resection while minimizing the amount of healthy tissue removed (*1*). The surgeon is provided with vital and real-time information on the location and extent of the lesion and can assess the resection margins. The technique uses a radiolabeled tracer preferentially taken up by the tumor to discriminate cancerous tissue from healthy organs, as well as a probe (*2*) sensitive to the emission released by the tracer to identify in real time the targeted tumor focus. The radiopharmaceutical is administered to the patient before surgery.

Current clinical applications of RGS are radioimmunoguided surgery for colon cancer (*3,4*), complete sentinel-node mapping for malignant melanoma (*5*) and breast cancer (*6,7*), and detection of parathyroid adenoma (*8*) and bone tumors (such as osteoid osteoma). There are also clinical studies on applications in neuroendocrine tumors (*9,10*).

Established methods use a combination of a $\gamma$-emitting tracer with a $\gamma$-radiation–detecting probe (*11,12*). Because $\gamma$ radiation can traverse large amounts of tissue, any uptake of the tracer in nearby healthy tissue represents a non-negligible background level, often preventing the use of this technique.

To overcome these limits and extend the range of RGS applications, it has been suggested (*13*) that pure $\beta^-$-emitting radioisotopes be used instead of $\gamma$-emitting tracers. $\beta^-$ radiation indeed penetrates only a few millimeters of tissue, with essentially no $\gamma$ contamination, since the bremsstrahlung contribution, which has a 0.1% emission probability, can be considered negligible. This novel approach allows development of a handy and compact probe, which, by detecting electrons and operating with a low radiation background, better delineates the margins of the lesion.

Received Jul. 24, 2014; revision accepted Nov. 10, 2014.
For correspondence or reprints contact: Riccardo Faccini, Universita' di Roma "La Sapienza," Piazzale Aldo Moro 2, 00185, Rome, Italy.
E-mail: riccardo.faccini@roma1.infn.it
Published online ••••••••••••.




jnm145995-sn ■ 12/9/14

This approach also requires less activity than traditional RGS approaches to detect tumor remnants, and because of the lower absorbed dose (*13*) and short range of electrons, the radiation exposure of medical personnel becomes almost negligible.

For this novel technique to be applicable, tracers capable of delivering pure $\beta^-$-emitting radionuclides are needed. Among the existing tracers, those used for molecular radiotherapy, in particular peptide receptor radionuclide therapy with $^{90}$Y, are the first candidates to be considered. Furthermore, neurosurgery is one of the fields that would profit most from RGS, given the importance of complete lesion removal. Finally, presurgical imaging is scarcely effective in the search for remnants because the operative field changes substantially during brain tumor resectioning. These considerations make $^{90}$Y-DOTATOC an optimal candidate tracer for a first application of RGS with $\beta^-$ radionuclides in brain tumors: meningioma has long been known to have substantial uptake of DOTATOC (*14–17*), and there are recent studies showing that high-grade glioma (HGG) also has somatostatin receptors (*18*).

Existing studies (*14*) focus on the uptake characteristics needed for molecular radiotherapy. This paper instead studies, in meningioma and HGG, aspects that are critical for RGS when the administered activities are significantly lower and the required tumor-to-nontumor ratio (TNR) is smaller.

## MATERIALS AND METHODS

### Estimate of DOTATOC Uptake

The first goal was to assess uptake of $^{90}$Y-DOTATOC in meningioma, HGG, and nearby healthy tissue. We have examined $^{68}$Ga-DOTATOC PET scans of the 2 diseases (*19*), with the reasonable assumption that gallium and yttrium are chemically similar enough not to alter the kinetics of the tracer. Patients were injected with a 3 MBq/kg dose of $^{68}$Ga-DOTATOC. After a 50-min uptake period, whole-body imaging was performed on a bismuth germanium oxide–equipped Discovery 600 PET/CT scanner (GE Healthcare) using a standard vertex-to-pelvis protocol. The CT acquisition protocol included low-dose CT (120 kV, automatic amperage, noise index $< 25$, pitch of 1.375, and 3.75-mm slice thickness) for attenuation correction followed by a whole-body PET scan (3 min per bed position). The PET scans were acquired in 3-dimensional mode in a $256 \times 256$ matrix (voxel size, $2.73 \times 2.73 \times 3.17$ mm). Images were reconstructed using VUE Point HD (GE Healthcare) attenuation-weighted ordered-subsets expectation maximization (2 iterations, 16 subsets) followed by a postreconstruction smoothing gaussian filter (5 mm in full width at half maximum).

We retrospectively analyzed, with AMIDE software, DICOM images of 11 patients with meningioma and 12 with HGG and estimated mean tumor uptake and uptake in nearby healthy tissues (the nontumor estimate needed to compute TNR). All patients gave written informed consent to participate in the clinical research, and the Ethics Committee (institutional review board) approved this retrospective

**TABLE 1**
Results for Meningioma Patients

| Patient no. | $N_{les.}$ | Weight (kg) | $A_{adm}$ (MBq) | $\nu^{*\dagger}$ (Hz) | $\nu_{NT}{}^{*\dagger}$ (Hz) | $t^{min}_{probe}{}^{*\dagger}$ (s) | $A^{min*}_{1s}$ (MBq/kg) | Diagnosis | Previous treatment |
|---|---|---|---|---|---|---|---|---|---|
| M01 | 1 | 63 | 220 | 32.2 | 1.9 | 0.2 | 0.7 | Atypical | S |
| M02 | 1 | 80 | 160 | 17.6 | 2.6 | 0.6 | 1.9 | Atypical | S/RT/PRRT |
| M03 | 3 | 95 | 305 | 33.7 | 3.5 | 0.3 | 0.9 | Likely atypical | S/RT |
| | | | | 50.3 | 3.5 | 0.3 | 0.5 | | |
| | | | | 76.8 | 3.5 | 0.1 | 0.3 | | |
| M04 | 1 | 48 | 200 | 89.4 | 4.5 | 0.1 | 0.2 | Atypical | S/RT/CT |
| M05 | 3 | 57 | 130 | 66.7 | 4.4 | 0.2 | 0.3 | Relapse | S/RT/CT/PRRT |
| | | | | 53.2 | 4.4 | 0.2 | 0.5 | | |
| | | | | 57.6 | 4.4 | 0.2 | 0.4 | | |
| M06 | 2 | 90 | 145 | 107.6 | 1.8 | 0.1 | 0.1 | Unknown | PRRT |
| | | | | 56.1 | 1.8 | 0.2 | 0.4 | | |
| M07 | 1 | 74 | 237 | 50.2 | 3.9 | 0.2 | 0.5 | Anaplastic | S/RT |
| M08 | 3 | 105 | 223 | 55.7 | 3.6 | 0.2 | 0.5 | Atypical | S/RT |
| | | | | 31.2 | 3.6 | 0.2 | 0.9 | | |
| | | | | 29.6 | 3.6 | 0.4 | 0.9 | | |
| M09 | 2 | 48 | 145 | 13.4 | 2.4 | 0.9 | 2.7 | Atypical | S/RT |
| | | | | 15.1 | 2.4 | 0.7 | 2.5 | | |
| M10 | 1 | 70 | 240 | 14.6 | 1.2 | 0.6 | 1.8 | Atypical | S/RT |
| | | | | 12.6 | 1.2 | 0.8 | 1.9 | | |
| M11 | 1 | 75 | 220 | 12.7 | 3.8 | 1.6 | 5.0 | Atypical | Unknown |

*Data assume 12 h between administration of $^{90}$Y and surgery.

†Estimations assume that reference activity $A_{ref} = 3$ MBq/kg is administered.

$N_{les.}$ = number of lesions; $A_{adm}$ = administered activity; $\nu$ = signal rate expected on probe in each lesion; $\nu_{NT}$ = nontumor rate expected on probe in each lesion; $t^{min}_{probe}$ = time needed to identify a 0.1-mL residual; $A^{min}_{1s}$ = the minimum activity that needs to be administered to have $t^{min}_{probe} = 1$ s; S = surgery; RT = radiotherapy; PRRT = peptide receptor radionuclide therapy; CT = chemotherapy.

**TABLE 2**
Results for HGG Patients

| Patient no. | Weight (kg) | $A_{adm}$ (MBq) | $\nu^{*\dagger}$ (Hz) | $\nu_{NT}{}^{*\dagger}$ (Hz) | $t^{min}_{probe}{}^{*\dagger}$ (s) | $A^{min*}_{1s}$ (MBq/kg) | Diagnosis | Previous treatment |
|---|---|---|---|---|---|---|---|---|
| G01 | 97 | 246 | 16.5 | 1.4 | 0.5 | 1.5 | HGG | S/RT/CT/PRRT |
| G02 | 68 | 223 | 5.2 | 1.1 | 2.6 | 8.5 | HGG | RT/CT/B |
| G03 | 80 | 152 | 9.6 | 1.9 | 1.4 | 4.3 | HGG | S/RT/CT |
| G04 | 93 | 198 | 22.4 | 3.7 | 0.6 | 1.8 | HGG | S/RT/CT/PRRT |
| G05 | 90 | 192 | 4.6 | 2.0 | 7.4 | 23.6 | HGG | S/RT/CT/PRRT |
| G06 | 60 | 185 | 4.4 | 1.6 | 5.8 | 20.0 | HGG | S/RT/CT |
| G07 | 63 | 194 | 4.8 | 1.7 | 5.1 | 17.6 | HGG | S/RT/CT |
| G08 | 70 | 266 | 2.1 | 0.8 | — | 40.0 | HGG | RT/CT |
| G09 | 85 | 255 | 3.7 | 1.1 | 5.3 | 17.6 | HGG | S/RT/CT |
| G10 | 80 | 224 | 2.2 | 1.6 | — | — | Oligodendroglioma | S/RT/CT/I |
| G11 | 70 | 234 | 5.1 | 2.0 | 5.5 | 18.8 | HGG | RT/CT |
| G12 | 15 | 38 | 5.0 | 2.0 | 5.9 | 18.8 | Pontine glioma | RT/CT/PRRT |

*Data assume 12 h between administration of $^{90}$Y and surgery.
†Estimations assume that reference activity $A_{ref}$ = 3 MBq/kg is administered.
$N_{les.}$ = number of lesions; $A_{adm}$ = administered activity; $\nu$ = signal rate expected on probe in each lesion; $\nu_{NT}$ = nontumor rate expected on probe in each lesion; $t^{min}_{probe}$ = time needed to identify a 0.1-mL residual; $A^{min}_{1s}$ = the minimum activity that needs to be administered to have $t^{min}_{probe}$ = 1 s; S = surgery; RT = radiotherapy; CT = chemotherapy; PRRT = peptide receptor radionuclide therapy; B = bevacizumab; I = immunotherapy.

[Table 1] [Table 2] study. The characteristics of the meningioma and HGG patients are summarized in Tables 1 and 2, respectively.

To estimate mean tumor uptake, for each meningioma patient we considered several PET slices and defined in each a region of interest (ROI) containing only lesioned tissue on the basis of the CT scans [Fig. 1] (Fig. 1, left). If there were several lesions, each was considered separately. In HGG, there was often a necrotic area between areas of uptake (center of Fig. 1) because of previous treatments. In such cases, an ROI comprehensive both of uptake areas and of interstitial areas was chosen.

[Fig. 2] For each of the $N_s$ slices (Fig. 2), the effective number of voxels $(N^v_i)$, the mean value $\mu_i$ ($i$ = 1, …, $N_s$), and the SD $\sigma_i$ of the voxel-specific activity were measured. From this information, the mean value of the tumor-specific activity $\mu$ and the corresponding uncertainty $\sigma_\mu$ was estimated with a weighted average:

$$\mu = \frac{\sum_i w_i \mu_i}{\sum_i w_i} \quad \sigma_\mu = \frac{1}{\sqrt{\sum_i w_i}}, \qquad \text{Eq. 1}$$

where $w_i = \frac{N^v_i}{\sigma^2_i}$.

[Fig. 3] Figure 3 shows typical values of $\mu_i$ for different slices and their average. Each slice in the DICOM images is 3.27 mm thick. The effects on the margins of the tumor are masked by the spatial resolution of approximately 3 mm. Such a resolution causes a systematic underestimation of the activity concentration, an effect known as the partial-volume effect. We conservatively avoided correcting for it.

To take into account differences in the activity administered to patients, the standardized uptake value (SUV) was estimated by normalizing the measured $\mu$ by the administered activity per unit of patient mass, after having rescaled this activity at the time of the PET scan:

$$\mathrm{SUV} = \frac{\mu W}{A_{adm} e^{-0.693 \Delta t_{PET} / T^{1/2}_{Ga}}}, \qquad \text{Eq. 2}$$

where $A_{adm}$ is the administered activity, $W$ the mass of the patient, $\Delta t_{PET}$ the elapsed time between administration and PET scan, and $T^{1/2}_{Ga}$ the $^{68}$Ga half-life.

RGB

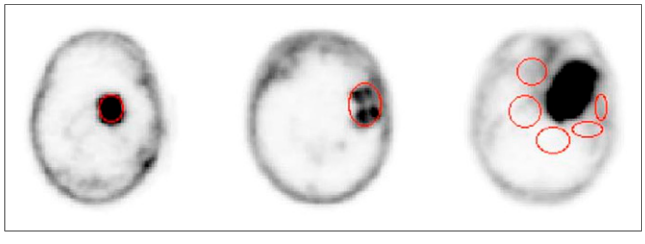

**FIGURE 1.** Example of ROI definition for meningioma (left), HGG (center), and nontumor (right).

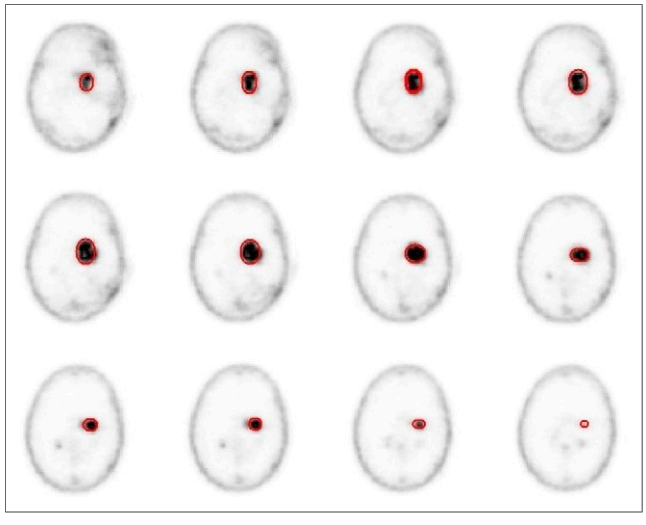

RGB

**FIGURE 2.** Example of ROI definition in several slices of PET scan of meningioma patient.



jnm145995-sn ■ 12/9/14

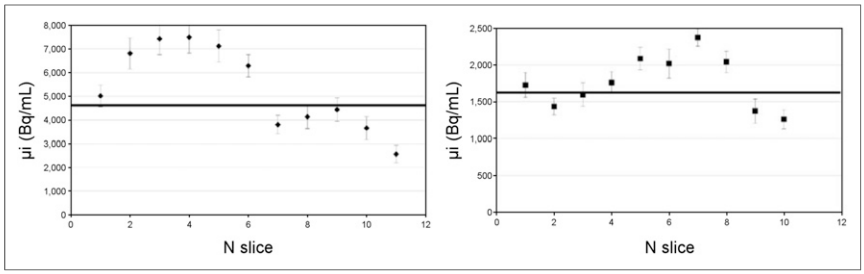


**FIGURE 3.** Example of $\mu_i$ estimated in different slices in case of meningioma (left) and glioma (right).

For healthy tissue, several ROIs on several slices of the scan were chosen. Because $\beta^-$ radiation is local, the ROIs were chosen by means of the CT information, close to the tumor margins, as shown in Figure 1 (right). A weighted average was used to evaluate $\mu_{NT}$, $\sigma_{NT}$, and the corresponding $SUV_{NT}$, where NT is normal tissue.

The TNR was estimated as the ratio between $\mu$ and $\mu_{NT}$.

### The $\beta^-$ Probe

A critical element in the development of the proposed RGS method is the $\beta^-$ probe, which exploits the low penetration power of the $\beta^-$ radiation by reducing the size of the lateral shielding. Furthermore, we found that we could minimize the sensitivity to $\gamma$ radiation using an organic scintillator with low density but high light yield (*p*-terphenyl (*20*)). The prototype used as the reference in this study has a sensitive cylinder of *p*-terphenyl with a radius of 2.55 mm and a [Fig. 4] 3-mm depth (Fig. 4). To maximize the accuracy of the direction of incoming radiation, the sensitive region is screened by 3 mm of polyvinyl chloride. The scintillation light is transported to a photomultiplier tube (Hamamatsu H10721-210 in the prototype) through 4 optical fibers.

### Expected Performance of RGS with $\beta^-$ Decays

From the measured specific activities, we also predicted the potential of RGS with $\beta^-$ decays. As previously detailed (*13*), this technique exploits the fact that more DOTATOC is taken up by tumor than by healthy tissues: the patient scheduled for surgery is injected, several hours in advance, with $^{90}$Y-DOTATOC. From the DICOM images, properly accounting for the radionuclide half-lives and assuming that administration of the radiotracer is $\Delta t_{surg} = 12$ h before the intervention, we can estimate the expected specific activity in tumor ($\mu^{ref}$) and nontumor ($\mu^{ref}_{NT}$) at the time of surgery for each patient:

$$\mu^{ref}_{(NT)} = SUV_{(NT)} A_{ref} e^{-0.693 \Delta t_{surg} / T_Y^{1/2}}, \quad \text{Eq. 3}$$

where $T_Y^{1/2}$ is the $^{90}$Y half-life. $A_{ref} = 3$ MBq/kg is a reference administered activity per unit mass, chosen as the activity injected for a typical PET scan.

After removing the bulk of the tumor, the surgeon explores the site with a $\beta^-$ probe to check the completeness of the resection. The probe responds to the presence of $\beta^-$ radiation with a signal whose rate ($\nu$) depends on the presence of radionuclides, their spatial distribution, and the probe characteristics. When the surgeon is probing for possible tumor residuals, a threshold on the number of counts in a given time interval has to be set to discriminate between healthy and lesion tissues.

To judge the feasibility of this approach, the measured specific activities $\mu^{ref}_{(NT)}$ need to be converted into the corresponding probe rates $\nu_{(NT)}$. To this aim, we performed a full simulation, including all interactions of particles with matter, using the FLUKA (*21,22*) Monte Carlo software. In this simulation, the background was represented by an extended region with a specific activity $\mu^{ref}_{NT}$ of $^{90}$Y, whereas the residual tumor used as a benchmark is a cylinder with a radius of 3 mm and a height of 3.5 mm for a total volume of 0.1 mL. These are indeed the dimension of typical residual tumor that has to be identified by the probe. The tumor region is assumed to have a specific activity $\mu^{ref}$ of $^{90}$Y.

The FLUKA software, fully simulating nuclear decay and the interactions between radiation and tissues, was used to estimate energy deposited inside the active volume of the probe by the emitted radiation. The conversion factor between the deposited energy and the electronic signal issued by the probe was determined in laboratory tests with a pointlike source of $^{90}$Sr of known activity. When the estimated electronic signal overcame a threshold that was determined in the same laboratory tests, the probe was considered to have issued a count.

From this simulation, we could then extract the signal rates that we expect to measure with a realistic $\beta^-$ probe in the presence of a tumor residual ($\nu$) or only healthy tissue ($\nu_{NT}$). These estimates, such as $\mu$ and $\mu_{NT}$, that are used as input depend on the administered activity of tracer.

From the measured detector rates we can estimate the time needed by the probe to identify a tumor residual of 0.1 mL with a given probability of false-positives or false-negatives. For a fixed acquisition time of the probe ($t_{probe}$) the false-positives and false-negatives are defined as follows:

$$\text{False-positive} = 1 - \sum_{N=0}^{N_{thr}-1} \mathscr{P}_{\nu_{NT} t_{probe}}(N) \quad \text{Eq. 4}$$

$$\text{False-negative} = \sum_{N=0}^{N_{thr}-1} \mathscr{P}_{\nu t_{probe}}(N), \quad \text{Eq. 5}$$

where $\mathscr{P}_\mu(N)$ indicates the Poisson probability of having $N$ if the mean is $\mu$, and $N_{thr}$ is the threshold in counts that we expect to set on the probe signal.

The minimum time that a surgeon needs to spend on a sample to evaluate whether it is healthy, $t^{min}_{probe}$, is determined by finding the minimal value of $t_{probe}$ for which there exists a value of $N_{thr}$ such that false-negatives are less than 5% and false-positives are less than 1%.

RGS can be practical only if, when the reference activity (3 MBq/kg) is administered, the time $t^{min}_{probe}$ is not significantly longer than


**FIGURE 4.** Photograph of probe prototype.

RGB



jnm145995-sn ■ 12/9/14

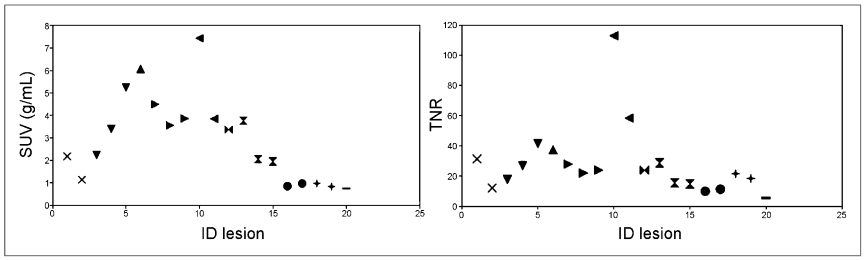


**FIGURE 5.** Measured SUV (left) and TNR (right) on all studied meningioma lesions. Lesions from same patient share same symbols. ID = sequential number identifying a lesion.

1 s—a reasonable time lapse in the surgical environment. Otherwise, an increase in activity would be needed. In contrast, if $t^{min}_{probe}$ is shorter than 1 s there are margins to reduce the administered activity. We therefore also calculated the minimum activity that needs to be administered ($A_{min}$) 12 h before surgery to achieve false-negatives less than 5% and false-positives less than 1% in $t^{min}_{probe} = 1$ s.

Scaling between activities neglects biologic washout from the organs. Nevertheless, washout is faster in healthy tissues than in tumors, which bind to the tracer. Tumors typically show constant or increasing uptake in the first day after administration and a washout after 24 h (*23,24*). Because the surgery, compared with the PET scan, takes place after a longer time has elapsed, the TNR was most likely underestimated and only conservative conclusions can be made about this study.

## RESULTS

Measurements on meningioma and HGG patients are shown in Tables 1 and 2.

### Meningioma Patients

The observed SUV and TNR for the meningioma patients is [Fig. 5] shown in Figure 5. About 70% of the lesions had an SUV greater than 2 g/mL, that is, administering 3 MBq/kg would yield a specific activity greater than 6 kBq/mL. The rest of the patients had an SUV of half this value. The TNR was greater than 10 in almost all cases and was usually above 20.

In terms of the feasibility of RGS with $\beta^-$ emitters, Table 1 reports for each patient the signal and nontumor rate expected on the probe; the time $t^{min}_{probe}$ needed to identify a 0.1-mL residual if an activity $A_{ref} = 3$ MBq/kg is administered; and the minimum activity, scaled to the time of the surgery, that needs to be administered to have $t^{min}_{probe} = 1$ s.

### HGG Patients

The measured SUV and TNR for the HGG patients is shown [Fig. 6] in Figure 6. About 60% of the lesions had an SUV of around 0.2 g/mL; that is, administering 3 MBq/kg would yield a specific activity of about 0.6 kBq/mL. The TNR was always at least 4 and was twice as high in a third of the cases. The only case in which uptake was marginal was the only oligodendroma in the sample.

We calculated the information relevant for RGS with $\beta^-$ decays (Table 2) and found that when 3 MBq/kg were administered, the probe required about 5–6 s in many cases to discriminate between lesion and healthy tissue. In such cases, to reduce the probing time to 1 s, a therapeutic activity of 20 MBq/kg would have to be administered.

## DISCUSSION

The novel RGS technique under development relies on the possibility of efficiently and selectively delivering a $\beta^-$ emitter. To this aim, this study examined uptake of $^{90}$Y-DOTATOC in 2 tumors of interest, meningioma and HGG.

Meningioma is known to have high receptivity to somatostatin analogs and therefore is ideal for testing the proposed technique. Nonetheless, it is important to determine whether there are meningioma patients who do not express enough receptors and what is the lowest administered activity for the technique to be effective, in order to minimize the exposure of patients and medical personnel. Only 1 of 11 meningioma patients did not express enough receptors to allow detection of a residual of 0.1 mL in less than 1 s. However, in that patient the probing time was less than 2 s. We can therefore conclude that the proposed RGS can be applied to all patients. Furthermore, in 60% of the patients the technique was estimated to be effective with administration of only 0.5 MBq/kg. Finally, the Monte Carlo approach developed here will be part of the protocol to determine the activity of $^{90}$Y-DOTATOC to administer to patients, since a $^{68}$Ga-DOTATOC PET scan will be acquired before surgery.

Regarding HGG, the literature has reported limited receptivity to DOTATOC. It was therefore important to ascertain whether uptake and TNR are sufficient for diagnostic use. Uptake was significantly less than for meningioma, but TNR was usually larger than 4, even with a conservative estimate. RGS with $\beta^-$ decays is thus expected to be reliable if each possible residual is examined for at most 5–6 s. Alternatively, to reduce the measurement time, the sensitivity of the probe can be improved: more sensitive devices can be used to collect scintillation light, and crystals with a larger light yield can be considered, although at the expense of having to develop a probe that requires more challenging engineering. Moreover, the estimates are conservative because regions between areas of good uptake are also included in the ROI since it cannot be established whether these regions represent tumor (Fig. 1).

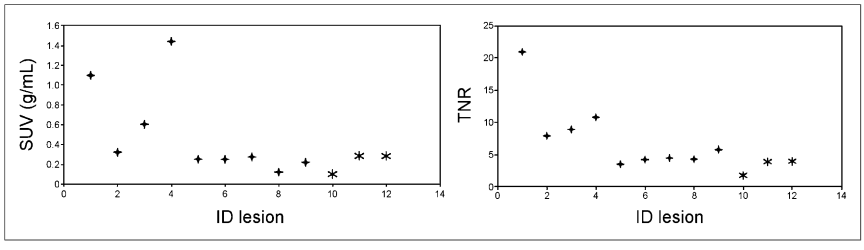


**FIGURE 6.** Measured SUV (left) and TNR (right) on all studied HGG lesions. ID = sequential number identifying a lesion.

## CONCLUSION

We estimated uptake of DOTATOC in meningiomas and HGGs in a feasibility study of a novel RGS technique exploiting $\beta^-$ decay. The results showed that, for



jnm145995-sn ■ 12/9/14

meningioma, the uptake is so marked that the technique can work even with administered activities much smaller than needed for PET scans. The minimum required activity can be computed on a patient-by-patient basis. The proposed technique can also work for HGG, although the more limited receptivity requires a longer probing time with the current version of the probe.

## DISCLOSURE

The costs of publication of this article were defrayed in part by the payment of page charges. Therefore, and solely to indicate this fact, this article is hereby marked "advertisement" in accordance with 18 USC section 1734. Fabio Bellini, Francesco Collamati, Erika De Lucia, Michela Marafini, Ilaria Mattei, Valerio Bocci, Luca Piersanti, Alessio Sarti, Adalberto Sciubba, Cecilia Voena, and Riccardo Faccini are listed as inventors on an Italian patent application (RM2013A000053) entitled "Utilizzo di radiazione beta− per la identificazione intraoperatoria di residui tumorali e la corrispondente sonda di rivelazione" and on the PCT patent application (PCT/IT2014/000025) entitled "Intraoperative detection of tumor residues using beta− radiation and corresponding probes," covering the method and instruments described in this paper. This study was financed by the research funds of the Università di Roma "La Sapienza." No other potential conflict of interest relevant to this article was reported.

## REFERENCES

1. Mariani G, Giuliano AE, Strauss HW. *Radioguided Surgery: A Comprehensive Team Approach.* New York, NY: Springer; 2006.
2. Hoffman EJ, Tornai MP, Janecek M, Patt BE, Iwanczyk JS. Intraoperative probes and imaging probes. *Eur J Nucl Med.* 1999;26:913–935.
3. Tiernan JP, Ansari I, Hirst NA, Millner PA, Hughes TA, Jayne DG. Intra-operative tumor detection and staging in colorectal cancer surgery. *Colorectal Dis.* 2012;14: e510–e520.
4. Filez L, Penninckx F, Ectors N, et al. Radioimmunoguided surgery for colorectal carcinoma. *Hepatogastroenterology.* 1999;46:691–700.
5. Manca G, Romanini A, Pellegrino D, et al. Optimal detection of sentinel lymph node metastases by intraoperative radioactive threshold and molecular analysis in patients with melanoma. *J Nucl Med.* 2008;49:1769–1775.
6. Angarita FA, Nadler A, Zerhouni S, Escallon J. Perioperative measures to optimize margin clearance in breast conserving surgery. *Surg Oncol.* 2014;23:81–91.
7. De Cicco C, Cremonesi M, Luini A, et al. Lymphoscintigraphy and radioguided biopsy of the sentinel axillary node in breast cancer. *J Nucl Med.* 1998;39:2080–2084.
8. Terzioğlu T, Senyurek YG, Tunca F, et al. Excision efficiency of radioguided occult lesion localization in reoperative thyroid and parathyroid surgery. *Thyroid.* 2010;20:1271–1278.
9. Gulec SA, Baum R. Radioguided surgery in neuroendocrine tumors using Ga-68-labeled somatostatin analogs. *J Surg Oncol.* 2007;96:309–315.
10. Kaemmerer D, Prasad V, Daffner W, et al. Radio-guided surgery in neuroendocrine tumors. *Clin Nucl Med.* 2012;37:142–147.
11. Tsuchimochi M, Hayamaand K. Intraoperative gamma cameras for radioguided surgery: technical characteristics, performance parameters, and clinical application. *Phys Med.* 2013;29:126–138.
12. Schneebaum S, Even-Sapir E, Cohen M, et al. Clinical applications of gamma-detection probes: radioguided surgery. *Eur J Nucl Med.* 1999;26(suppl):S26–S35.
13. Solfaroli Camillocci E, Baroni G, Bellini F, et al. A novel radioguided surgery technique exploiting $\beta^-$ decays. *Sci Rep.* 2014;4:4401.
14. Reubi JC, Maurer R, Klijn JGM, et al. High incidence of somatostatin receptors in human meningiomas: biochemical characterization. *J Clin Endocrinol Metab.* 1986;63:433–438.
15. Heppeler A, Froidevaux S, Macke HR, et al. Radiometal-labeled macrocyclic chelator-derivatised somatostatin analogue with superb tumor-targeting properties and potential for receptor-mediated internal radiotherapy. *Chem Eur J.* 1999;7:1974–1981.
16. De Jong M, Valkema R, Jamar F, et al. Somatostatin receptor-targeted radionuclide therapy of tumors: preclinical and clinical findings. *Semin Nucl Med.* 2002;32:133–140.
17. Bartolomei M, Bodei L, De Cicco C, et al. Peptide receptor radionuclide therapy with $^{90}$Y-DOTATOC in recurrent meningioma. *Eur J Nucl Med Mol Imaging.* 2009;36:1407–1416.
18. Heute D, Kostron H, von Guggenberg E, et al. Response of recurrent high-grade glioblastoma to treatment with $^{90}$Y-DOTATOC. *J Nucl Med.* 2010;51:397–400.
19. Henze M, Schuhmacher J, Hipp P, et al. PET imaging of somatostatin receptors using [$^{68}$GA]DOTA-D-Phe$^1$-Tyr$^3$-octreotide: first results in patients with meningiomas. *J Nucl Med.* 2001;42:1053–1056.
20. Angelone M, Battistoni G, Bellini F, et al. Properties of para-terphenyl as detector for alpha, beta and gamma radiation. *IEEE Trans Nucl Sci.* 2014;61:1483–1487.
21. Battistoni G. The FLUKA code [abstract]. *AIP Conf Proc.* 2007;896:31.
22. Ferrari A, Sala PR, Fassò A, Ranft J. *FLUKA: A Multi Particle Transport Code.* Geneva, Switzerland: CERN; 2005. Technical Report CERN-2005-10, INFN/TC05/11, SLAC-R-773.
23. Sward C, Bernhardt P, Johanson V, et al. Comparison of [$^{177}$Lu-DOTA0,Tyr3]-octreotate and [$^{177}$Lu-DOTA0,Tyr3]-octreotide for receptor-mediated radiation therapy of the xenografted human midgut carcinoid tumor GOT1. *Cancer Biother Radiopharm.* 2008;23:114–120.
24. Cremonesi M, Ferrari M, Zoboli S, et al. Biokinetics and dosimetry in patients administered with $^{111}$In-DOTA-Tyr$^3$-octreotide: implications for internal radiotherapy with $^{90}$Y-DOTATOC. *Eur J Nucl Med.* 1999;26:877–886.